Citation: CPT Pharmacometrics Syst. Pharmacol. (2016) 5, 264–273; doi:10.1002/psp4.12079


ORIGINAL ARTICLE

# Application of the Multistate Tuberculosis Pharmacometric Model in Patients With Rifampicin-Treated Pulmonary Tuberculosis

RJ Svensson* and USH Simonsson

**This is the first clinical implementation of the Multistate Tuberculosis Pharmacometric (MTP) model describing fast-, slow-, and nonmultiplying bacterial states of *Mycobacterium tuberculosis*. Colony forming unit data from 19 patients treated with rifampicin were analyzed. A previously developed rifampicin population pharmacokinetic (PK) model was linked to the MTP model previously developed using *in vitro* data. Drug effect was implemented as exposure-response relationships tested at several effect sites, both alone and in combination. All MTP model parameters were fixed to *in vitro* estimates except $B_{max}$. Drug effect was described by an on/off effect inhibiting growth of fast-multiplying bacteria in addition to linear increase of the stimulation of the death rate of slow- and nonmultiplying bacteria with increasing drug exposure. Clinical trial simulations predicted well three retrospective clinical trials using the final model that confirmed the potential utility of the MTP model in antitubercular drug development.**
*CPT Pharmacometrics Syst. Pharmacol.* (2016) **5**, 264–273; doi:10.1002/psp4.12079; published online 17 May 2016.

## Study Highlights

WHAT IS THE CURRENT KNOWLEDGE ON THE TOPIC? ☑ There is a lack of semimechanistic PK/PD models within TB. The MTP model has been applied to *in vitro* and animal data in which natural growth and rifampicin drug effect were successfully described. • WHAT QUESTION DID THIS STUDY ADDRESS? ☑ Can the MTP model be applied to clinical CFU data after rifampicin monotherapy? Can the approach predict retrospective clinical data using clinical trial simulations? • WHAT THIS STUDY ADDS TO OUR KNOWLEDGE ☑ The MTP model was successfully applied, which indicates that the MTP model can be used for clinical and preclinical trial simulation. In addition, this study adds to the evidence concerning rifampicin mechanism of action. • HOW THIS MIGHT CHANGE CLINICAL PHARMACOLOGY AND THERAPEUTICS ☑ The MTP model can potentially aid in decision support for trial designs and program design evaluations within the field of TB drug development.

Rifampicin is a recommended first-line antitubercular drug used in patients with drug-susceptible pulmonary tuberculosis (TB)[1] partly because rifampicin is efficient in avoiding relapse.[2] Rifampicin inhibits bacterial DNA-dependent RNA polymerase,[3,4] which is essential for bacterial metabolism, leading to activity against multiplying and nonmultiplying bacteria.[5]

Clinical symptoms appear late in the infection[6] when infections are at a stationary phase in which no change in the colony forming unit (CFU) over time in untreated patients is seen.[7] Studies on clinical sputum samples with resuscitation-promoting factors revealed that only 0.01–20% of *Mycobacterium tuberculosis* (*M. tuberculosis)* cells are quantified as CFU,[8] suggesting existence of a large portion of noncultivable nonmultiplying bacteria.

In short-term clinical data, a biexponential pattern of decline in CFU can be seen.[9] This is thought to be due to subpopulations with different drug susceptibility giving rise to an initial rapid and a late slower decline, respectively. The CFU readout is widely used within TB drug development to quantify treatment progression[10] in which the rate of decline in CFU is associated with treatment outcome.[11] *In vitro*, at least three different subpopulations exist within a *M. tuberculosis* culture.[12] Susceptibility relates to *in vitro* conditions; log-phase and oxygen-rich cultures are susceptible to drugs, whereas stationary phase and oxygen-poor cultures are not. Subpopulations surviving drug exposure are by definition phenotypically tolerant[13] and are slow- or nonmultiplying.[14]

The Multistate Tuberculosis Pharmacometric (MTP) model is a semimechanistic model describing fast-, slow-, and nonmultiplying bacteria. It has been successfully applied to describe *in vitro*[15] and mouse data[16] but not until now to clinical data.

The objective of the analysis was to apply the MTP model, linked to rifampicin pharmacokinetics (PKs), to clinical phase IIa CFU data in patients with drug-susceptible pulmonary TB. In addition, we performed clinical trial simulations using the developed final model in order to predict retrospective clinical data as external validation.

## METHODS

### Patients and study design

Data included individual sputum CFU counts from 23 patients with treatment-naive Kenyan drug-susceptible pulmonary TB divided into four arms: (1) no treatment

Department of Pharmaceutical Biosciences, Uppsala University, Uppsala, Sweden. *Correspondence: RJ Svensson (robin.svensson@farmbio.uu.se)
Received 29 December 2015; accepted 30 March 2016; published online on 17 May 2016. doi:10.1002/psp4.12079

(negative control, $n = 4$); (2) 5 mg/kg ($n = 3$); (3) 10 mg/kg ($n = 8$); or (4) 20 mg/kg ($n = 8$) rifampicin daily at 8 AM. Patients were treated for 14 days with sputum collected during 12 hours overnight (between 8 PM and 8 AM) every second day, including two baseline measurements. Sputum samples were cultivated on agar plates for CFU counting. For more details, the reader is referred to the original publication.[17] No formal ethical review boards or written consent process existed at the time of the conduct of the study (1966–1977). However, the principal investigator has confirmed that no restrictions relating to reuse of data were envisaged and reuse of the irreversibly anonymized data by the PreDiCT-TB consortium was approved by the UK National Research Ethics Service.

**Overall modeling strategy**

The first step was to adapt the MTP model[15] for the clinical TB setting. This was done by fixing all parameters except $B_{max}$ to estimates from the *in vitro* MTP setting.[15] The second step was to include a human rifampicin PK model in order to describe rifampicin exposure. Finally, drug effect was quantified by developing exposure-response relationships linking the PK model to the MTP (disease) model. All observed CFU data were modeled simultaneously as the natural logarithm of CFU in $ml^{-1}$ and log-transformation both sides. Data analysis was performed with the nonlinear mixed effects modeling software NONMEM version 7.3 (Icon Development Solutions [http://www.iconplc.com/technology/products/nonmem], Ellicott City, MD)[18] using the first-order conditional estimation with interaction. Data handling was performed in R version 3.1.1 (R Foundation for Statistical Computing [http://www.R-project.org], Vienna, Austria).

**Population pharmacokinetic model**

As previously described, the PK-enzyme turnover model for rifampicin[19] was used as the PK model. Because the data contained no observed rifampicin concentrations, a population PK parameter approach[20] was used. Random variability parameters were removed with the remaining structural parameters fixed to reported estimates of fixed effects. As no covariate information was available, covariates were set to most common or median values. Each patient was assumed to be human immunodeficiency virus (HIV) negative with a body weight of 56 kg and a fat free mass of 45 kg, which were the mean observed demographics in the study used for developing the PK model.[19] These patients originated from South Africa, Senegal, Benin, and Guinea.

**The Multistate Tuberculosis Pharmacometric model**

The structure of the MTP model[15] developed using *in vitro* time-kill data was used as the disease model. The structure included fast-multiplying, slow-multiplying, and nonmultiplying bacterial states. Only the bacterial numbers in the fast- and slow-multiplying states were visible as CFU, the nonmultiplying state was considered nonculturable. Growth of the fast-multiplying state was described by a Gompertz function. The MTP model does not include growth of slow-multiplying bacteria but only increase of slow-multiplying bacteria because of transfer of bacteria from the fast-multiplying state.[15] Each bacterial substate was allowed to transfer between all states, except from non- to fast-multiplying state. This transfer was judged scientifically negligible *in vitro* because of hypoxia.[15] The transfer rate from fast- to slow-multiplying state increased linearly with time.

The differential equations were written as:

$$\frac{dF}{dt} = k_G \cdot \log\left(\frac{B_{max}}{F+S+N}\right) \cdot F + k_{SF} \cdot S - k_{FS} \cdot F - k_{FN} \cdot F$$

$$\frac{dS}{dt} = k_{FS} \cdot F + k_{NS} \cdot N - k_{SF} \cdot S - k_{SN} \cdot S$$

$$\frac{dN}{dt} = k_{FN} \cdot F + k_{SN} \cdot S$$

where $k_{FS} = k_{FS_{lin}} \cdot t$ where F, S, and N are the model predicted bacterial number ($ml^{-1}$) in fast-, slow-, and nonmultiplying states, respectively. Various k with two-letter subscripts are transfer rates between substates. The first letter describes the transfer origin and the second letter describes the direction. The parameter $k_{FSlin}$ multiplied by time (t) in days after infection describes the time-dependent transfer rate from fast- to slow-multiplying state. The parameter $k_G$ is the fast-multiplying bacterial growth rate and $B_{max}$ is the system carrying capacity, constraining the growth in the stationary phase.

In order to evaluate the importance of the nonmultiplying substate in the MTP model, an alternative two-state model not including a nonmultiplying state was developed. The differential equations for the two-state model were written as:

$$\frac{dF}{dt} = k_G \cdot \log\left(\frac{B_{max}}{F+S}\right) \cdot F + k_{SF} \cdot S - k_{FS} \cdot F - k_D \cdot F$$

$$\frac{dS}{dt} = k_{FS} \cdot F - k_{SF} \cdot S - k_D \cdot S$$

where $k_{FS} = k_{FS_{lin}} \cdot t$ where $k_D$ is the natural death rate in $days^{-1}$, needed to adequately describe the CFU *in vitro* data when assuming no nonmultiplying state.[15] The CFU declines at ~70 days, which is correctly described as a shift into the nonmultiplying state in the MTP model but is described as natural death in the alternative two-state model. The parameters of the two-state model were estimated using the same *in vitro* data as was used to develop the structure of the MTP model.[15] All model fitting and assumptions were otherwise similar as for the MTP model.

All patients were assumed to have stationary phase infections. Time from inoculum (i.e., infection) to stationary phase for the *in vitro* MTP model[15] was investigated through simulations in Berkeley Madonna version 8.3.18 (Department of Molecular and Cellular Biology, University of California [http://www.berkeleymadonna.com], Berkeley, CA). Simulations in Berkeley Madonna were also used to assess identifiability of parameters suitable for estimation and corresponding impact on CFU vs. time.

Drug effect using the clinical data was investigated in four sequential steps. The first step investigated drug effect on different effect sites as univariate (i.e., single effect site) models. Effect site refers to either inhibition of fast-multiplying growth or stimulation of fast-, slow-, or nonmultiplying death in the MTP model. Included models were on/

off (constant maximal drug effect at drug concentrations above 0 mg/L), linear, $E_{max}$, and sigmoidal $E_{max}$ models. Drug effects were incorporated as:

$$\frac{dF}{dt} = k_G \cdot \log\left(\frac{B_{max}}{F+S+N}\right) \cdot F \cdot (1-EFF_{FG}) + k_{SF} \cdot S - k_{FS} \cdot F - k_{FN} \cdot F - EFF_{FD} \cdot F$$

$$\frac{dS}{dt} = k_{FS} \cdot F + k_{NS} \cdot N - k_{SF} \cdot S - k_{SN} \cdot S - EFF_{SD} \cdot S$$

$$\frac{dN}{dt} = k_{FN} \cdot F + k_{SN} \cdot S - k_{NS} \cdot N - EFF_{ND} \cdot N$$

where $EFF_{FG}$, $EFF_{FD}$, $EFF_{SD}$, and $EFF_{ND}$ are the drug effects as inhibition of fast-multiplying growth and death of fast-, slow-, and nonmultiplying, respectively. Models were statistically significant at 5% significance level if the objective function value (OFV) decreased by at least 3.84 ($\chi^2$ distribution) for nested models with addition of one parameter. The second step investigated effect sites in combination. To not exclude effect sites that were apparent only in combination, all effect sites were included. In addition, to not exclude any exposure-response relationships, all effect sites included at least linear models. All combinations of effect sites were tested. The statistically significant combination that fitted the data best (i.e., lowest OFV) was selected. The third step reevaluated the exposure-response relationship at each effect site. All drug effect models were retested at each effect site. If an alternative drug effect model was statistically significant on one effect site, that model was kept. If multiple effect sites had statistically significant alternative drug effect models, the model with the best model fit (i.e., lowest OFV) was kept and tested for statistical significance in combination with the model with the second best model fit until no alternative model was supported. The fourth step was a backward elimination step at 1% significance level ($\Delta$OFV $\geq$6.63 for removal of one parameter). Each effect site was removed to exclude nonsignificant effect sites at 1% significance level, resulting in a full model.

Three approaches to handle predictions of CFU were evaluated. For the last time point method, predictions were defined as the bacterial number in the fast- and slow-multiplying states per milliliter sputum at the last time point of the sputum sampling interval, which was at 8 AM because all samples were collected between 8 PM and 8 AM. For the mid-time point method, predictions were defined as the bacterial number in the fast- and slow-multiplying states in $mL^{-1}$ at the mid-point in the sputum sampling period (2 AM). The time for each observation was for both methods specified in the dataset. Predictions of CFU were defined as:

$$PRED = \log(F+S)$$

where PRED is the prediction of the natural logarithm of F and S in $mL^{-1}$.

For the sputum sampling compartment method, predictions were defined as the average bacterial number in the fast- and slow-multiplying states ($mL^{-1}$) in the sputum sampling interval (between 8 PM and 8 AM). This was implemented by inclusion of a sputum sample compartment described by:

**Table 1** Overview of trials included in external validation

| Dose arm | Location | Ethnicities | Age | Comorbidities | Study arm size | Study length | Sputum sampling | Publication year | Reference |
|---|---|---|---|---|---|---|---|---|---|
| 600 mg | South Africa | 57% black[a] | Median 34 y, range 18–61 y[a] | 31% HIV-positive[a] | 15 | 7 d | Baseline and d 1, 2, 3, 4, 5, 6, and 7 | 2008 | 26 |
| 20 mg/kg | South Africa | No information available in publication | Mean 27 y, SD 9 y | 23% HIV-positive | 13 | 5 d | Baseline and d 1, 2, 3, 4, and 5 | 2007 | 27 |
| 300 mg | South Africa | No information available in publication | No information available in publication | 24% HIV-positive[a] | 16 | 5 d | Baseline and d 2 and 5 | 2005 | 28 |
| 600 mg | South Africa | No information available in publication | No information available in publication | 24% HIV-positive[a] | 14 | 5 d | Baseline and d 2 and 5 | 2005 | 28 |

HIV, human immunodeficiency virus.
[a]For the whole trial and not the rifampicin arm specifically.

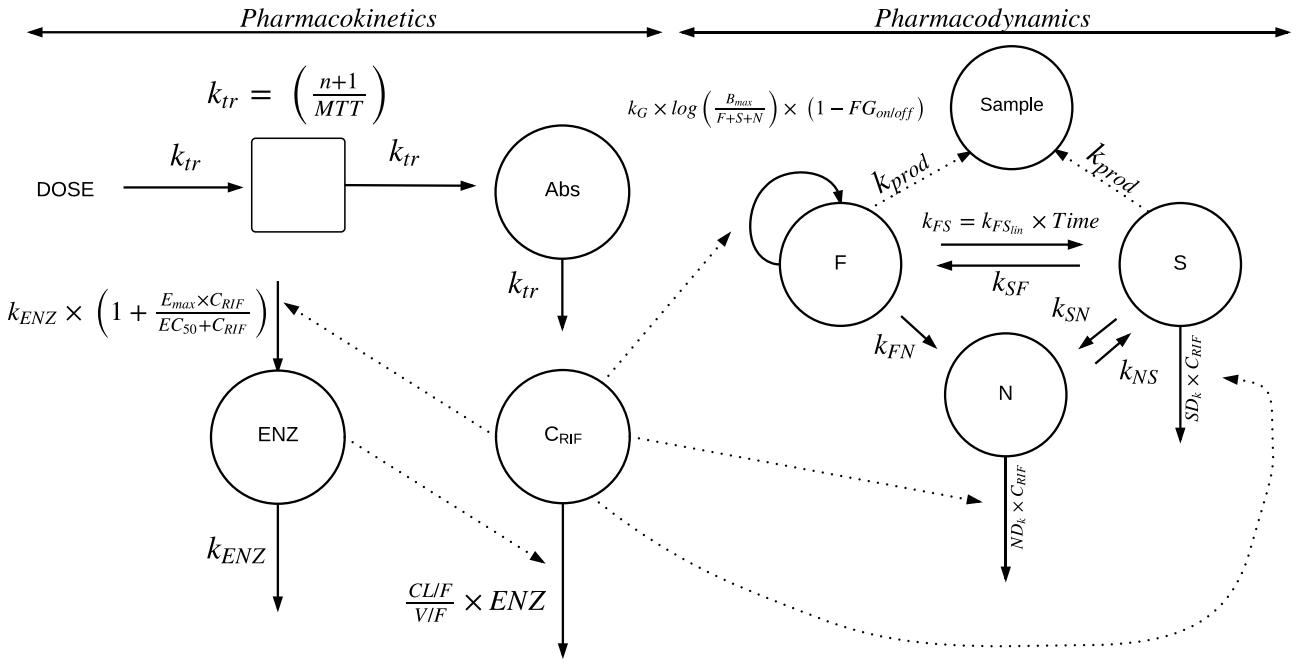


**Figure 1** Schematic describing the final model. The dose (DOSE) is transferred from the absorption site (Abs) to the central compartment by a transit rate constant $k_{tr}$, which is described by the number of compartments (n) +1 divided by the mean transit time (MTT). Drug is eliminated linearly as described by rifampicin oral clearance (CL/F) divided by the apparent volume of distribution (V/F), at the preinduced stage. The pharmacokinetic (PK) model includes an enzyme turnover model, in which plasma concentrations of rifampicin ($C_{RIF}$) increase the rate constant for first-order degradation of the enzyme pool ($k_{ENZ}$), which leads to an increase in the enzyme pool (ENZ) with an $E_{max}$ model leading to increased elimination of rifampicin. The parameter $EC_{50}$ is the rifampicin concentration ($C_{RIF}$) at which half the $E_{max}$ is reached. $E_{max}$ is the maximal increase in the enzyme production rate. $C_{RIF}$ drives the effect implemented in the Multistate Tuberculosis Pharmacometric (MTP) model. The MTP model consists of three bacterial compartments; the fast-multiplying state (F), the slow-multiplying state (S), and the nonmultiplying state (N). Growth is present for F described by a fast-multiplying bacterial growth rate ($k_G$) multiplied by the natural logarithm of the system carrying capacity per milliliter sputum ($B_{max}$) divided by the number of F, S, and N. F can transfer to N described by the transfer rate from fast- to nonmultiplying state ($k_{FN}$). Transfer between F and S is described by a time-dependent transfer rate from fast- to slow-multiplying state ($k_{FSlin}$). S can transfer to F and N described by the transfer rate from slow- to fast-multiplying state ($k_{SF}$) and transfer rate from slow- to nonmultiplying state ($k_{SN}$), respectively. N can transfer to S described by the transfer rate from non- to slow-multiplying state ($k_{NS}$). Drug effect enters the model as fractional inhibition of growth of fast-multiplying state ($FG_{on/off}$) in presence of drug according to the PK model, as second-order nonmultiplying death rate ($ND_k$) and as second-order slow-multiplying death rate ($SD_k$). The bacterial number of F and S together with the sputum production rate ($k_{prod}$) describes the amount of bacteria that is present in the sputum sample compartment (Sample).

$$\frac{dSample}{dt} = k_{prod} \cdot (F+S)$$

where $k_{prod} = \frac{V_{sputum}}{D_{sample}}$ Sample is the bacterial number in the fast- and slow-multiplying states in the specified sputum volume over the sampling interval. The sputum production rate is $k_{prod}$ (mL/h). Sputum volume is $V_{sputum}$ (mL) and the sampling duration is $D_{sample}$ (hours). The amount in the sample compartment was set to 0 at the start of each collection period. Predictions of CFU were defined as:

$$PRED = log\left(\frac{Sample}{V_{sputum}}\right)$$

where PRED is the natural logarithm of the average bacterial number in the fast- and slow-multiplying states ($mL^{-1}$) over the sampling interval. The true sample volume was unavailable in this study and was assumed to be 10 mL for all samples, a realistic value based on reported sputum volumes.[21] Start and duration of sputum sample collection and sample volume were specified in the dataset (**Supplementary Material S1**).

Attempts were made to model immune response implemented as specific zero- and first-order death rates on the fast-, slow-, and nonmultiplying states. Furthermore, effect delay models, implemented as effect compartment models, were tested on all effect sites.

Random effects were tested in $B_{max}$. Interindividual variability (IIV) was parameterized as:

$$P = TVP \times e^{\eta}$$

where P is the parameter, TVP is the typical value of the parameter, and $\eta$ is a normally distributed parameter. Error models implemented as additive error on log scale (approximates proportional error on normal scale) and combined errors (including two additive errors; one on normal scale and one on log scale) were tested.

Observed CFU values were reported in replicate and analyzed without averaging. To avoid bias because of correlation between replicates a residual error model with two components, one where the error was similar for all replicates and one where the error was the same for replicates

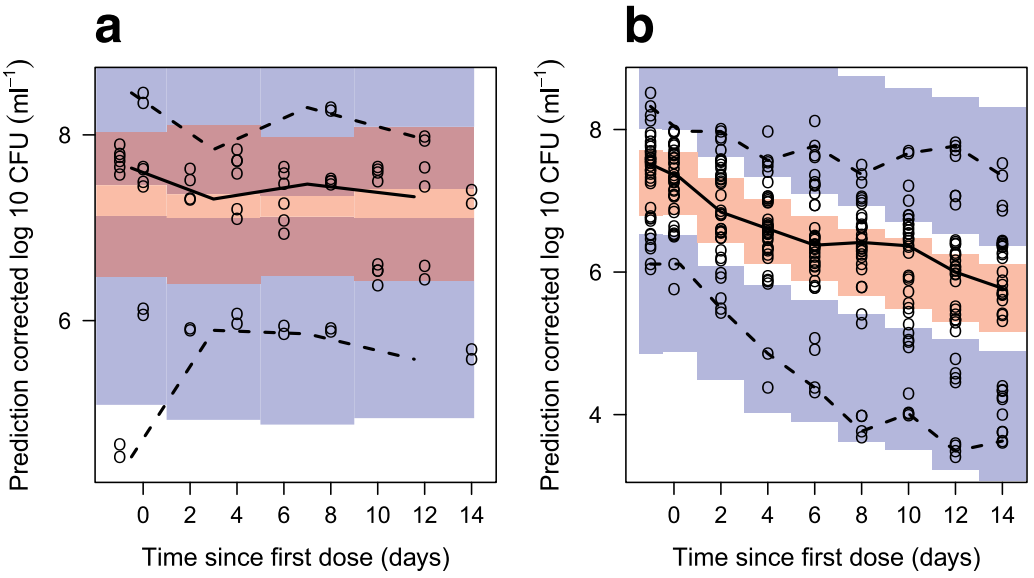


**Figure 2** Prediction-corrected visual predictive check of the final model stratified on presence of drug in which (**a**) is the group that received no drug and (**b**) is all groups that received drug. The solid and dashed lines are the median, 2.5th, and 97.5th percentiles of the observed data, respectively. The shaded areas (top to bottom) are the 95% confidence intervals of the 97.5th (blue), median (red), and 2.5th (blue) percentiles of the simulated data. Open circles are prediction-corrected observations.

from the same sputum sample, were tested. This was implemented using the L2 data item in NONMEM. No data were below the limit of quantification.

### Model selection and evaluation

Models were evaluated by comparing the difference in OFV together with parameter precision and diagnostic plots generated with the R package Xpose version 4.5.2 (Department of Pharmaceutical Biosciences, Uppsala University [http://xpose.sourceforge.net], Uppsala, Sweden).[22,23] In addition, prediction-corrected visual predictive checks[24] were generated using PsN version 4.3.2 (Department of Pharmaceutical Biosciences [http://psn.sourceforge.net])[22,25] using 1,000 simulations. A prediction-corrected visual predictive check normalizes the observed and simulated dependent variable to the median typical prediction within each bin, allowing visual interpretation of several doses in one plot, which is not always the case with a traditional visual predictive check.[22,25] A 1,000 sample bootstrap was performed in PsN[22,25] on the final model in order to obtain the nonparametric 95% confidence interval for all estimated parameters.

### Clinical trial simulations

External validation was performed by comparing model predicted 95% prediction intervals (PIs) of the typical change in CFU from baseline vs. time to the mean ± SE of four datasets not used for model building. The datasets consisted of rifampicin in monotherapy with different doses and study lengths,[26–28] summarized in **Table 1**. The PI of the typical predictions was generated from 1,000 samples simulated with uncertainty in parameter estimates.

## RESULTS

The final MTP model had the same structure as the final MTP model developed using *in vitro* data,[15] as shown in **Figure 1**. An example dataset and final model code are found in **Supplementary Material S1 and S2**, respectively. Simulations from the MTP model developed using *in vitro* data[15] revealed that stationary phase was apparent beyond 130 days after infection. Because all patients were assumed to have stationary phase infections, time for start of treatment was set to 150 days after infection for all patients.

The OFV was lower ($\Delta OFV = -4.19$) for the final MTP model compared to the two-state model without nonmultiplying state, which indicates a better fit.

All MTP model parameters were fixed to *in vitro* estimates,[15] except for $B_{max}$, which was estimated. Using the *in vitro* $B_{max}$ value resulted in an increase in OFV by 53.2 and predicted typical log-10 CFU at day 150 of 6.23 $mL^{-1}$, whereas the mean observed baseline value in the clinical dataset was 7.64 $mL^{-1}$. Simulations with different values for $B_{max}$ yielded identical relative amounts of bacterial states at stationary phase because transfer rates between states were fixed. Parameters $k_G$, $k_{FSlin}$, $k_{SF}$, $k_{SN}$, $k_{NS}$, and $k_{FN}$ were unidentifiable. This was probably because of the short study duration and that data were obtained at a stationary phase of infection. Regardless, fixing these parameters to *in vitro* estimates provided a good fit to the observed data (**Figure 2**).

Statistically significant exposure-response relationships were found between drug exposure and inhibition of the growth rate of the fast-multiplying state and stimulation of the death rates of the slow- and nonmultiplying states (**Figure 1**). The data did not support any statistically

**Table 2** Parameter estimates based on the final model

| Parameter | Description | Typical estimate | RSE%[a] | 95% CI[b] |
|---|---|---|---|---|
| Drug PK parameters[c] | | | | |
| CL/F ($L \cdot h^{-1}$) | Oral clearance at the preinduced state in a patient weighing 70 kg | 10.0 FIX | - | - |
| V/F (L) | Apparent volume of distribution in a patient weighing 70 kg | 86.7 FIX | - | - |
| MTT (h) | Mean transit time | 0.713 FIX | - | - |
| NN | Number of transit compartments | 1.00 FIX | - | - |
| $E_{max}$ | Maximal increase in the enzyme production rate | 1.04 FIX | - | - |
| $EC_{50}$ ($mg \cdot L^{-1}$) | Rifampicin concentration at which half the $E_{max}$ is reached | 0.0705 FIX | - | - |
| $k_{ENZ}$ ($h^{-1}$) | Rate constant for first-order degradation of the enzyme pool | 0.00369 FIX | - | - |
| F | Bioavailability | 1.00 FIX | - | - |
| $(Ffat)_{CL/F}$ | Contribution of fat-free mass and body weight to CL/F | 0.311 FIX | - | - |
| $(Ffat)_{V/F}$ | Contribution of fat-free mass and body weight to V/F | 0.188 FIX | - | - |
| Multistate Tuberculosis Pharmacometric model[d] | | | | |
| $k_G$ ($days^{-1}$)[e] | Fast-multiplying bacterial growth rate | 0.206 FIX | - | - |
| $k_{FN}$ ($days^{-1}$) | Transfer rate from fast- to nonmultiplying state | $8.97 \cdot 10^{-7}$ FIX | - | - |
| $k_{SN}$ ($days^{-1}$) | Transfer rate from slow- to nonmultiplying state | 0.186 FIX | - | - |
| $k_{SF}$ ($days^{-1}$) | Transfer rate from slow- to fast-multiplying state | 0.0145 FIX | - | - |
| $k_{NS}$ ($days^{-1}$) | Transfer rate from non- to slow-multiplying state | 0.00123 FIX | - | - |
| $k_{FSlin}$ ($days^{-2}$)[f] | Time-dependent transfer rate from fast- to slow-multiplying state | 0.00166 FIX | - | - |
| $F_0$ ($mL^{-1}$) | Initial bacterial number of fast-multiplying state | 4.10 FIX | - | - |
| $S_0$ ($mL^{-1}$) | Initial bacterial number of slow-multiplying state | 9770 FIX | - | - |
| $B_{max}$ ($mL^{-1}$)[d] | System carrying capacity per mL sputum | $2.61 \cdot 10^9$ | 30.5 | $1.51 \cdot 10^9 - 4.52 \cdot 10^9$ |
| IIV $B_{max}$ (%)[g] | Interindividual variability in $B_{max}$ | 152 | 15.9 | 97.8–191 |
| Exposure-response parameters | | | | |
| $FG_{on/off}$ | Fractional inhibition of growth of fast-multiplying state | 1.00 FIX | - | - |
| $SD_k$ ($L \cdot mg^{-1} \cdot days^{-1}$) | Second-order slow-multiplying state death rate | 0.200 | 41.6 | 0.0854–0.390 |
| $ND_k$ ($L \cdot mg^{-1} \cdot days^{-1}$) | Second-order nonmultiplying state death rate | 0.106 | 19.0 | 0.0643–0.188 |
| Residual error parameters | | | | |
| $\varepsilon$ (CV%) | Additive residual error on log scale (approximates a proportional error on normal scale) for all replicates | 110 | 12.0 | 83.7–133 |
| $\varepsilon_{repl}$ (CV%) | Additive residual error on log scale (approximates a proportional error on normal scale) between replicates | 23.1 | 10.2 | 18.4–27.2 |

CI, confidence interval; FIX, parameter was fixed during estimation; PK, pharmacokinetic; RSE, relative standard error.
[a]Relative standard error from the covariance step in NONMEM[18] reported on the approximate SD scale.
[b]95% CI is the 95% percentile confidence interval from a nonparametric bootstrap (1,000 samples).
[c]All drug PK model parameters were fixed to estimates reported by Smythe *et al.*[19]
[d]All Multistate Tuberculosis Pharmacometric Model parameters except $B_{max}$ were fixed to estimates reported by Clewe *et al.*[15]
[e]$\frac{dF}{dt} = k_G \cdot \left(\frac{B_{max}}{F+S+N}\right) \cdot F$
[f]$k_{FS} = k_{FSlin} \cdot t$
[g]IIV is the inter-individual variability expressed as coefficient of variation (CV).

significant exposure-response relationship concerning death of the fast-multiplying state. Inhibition of the growth rate of the fast-multiplying state was described by an on/off effect. Drug effects on the slow- and nonmultiplying states were described by second-order death rates, denoted $SD_k$ and $ND_k$, respectively. The second-order rates were dependent on the plasma concentration of rifampicin and amount of bacteria (slow- or nonmultiplying).

The sputum sampling compartment method was chosen to handle CFU predictions. The last time point and mid-time point methods provided similar OFV, but was regarded to not resemble the actual sample collection procedure. The data did not support any statistically significant effect delay or immune response.

The data supported IIV in $B_{max}$, which allowed for prediction of different baseline levels in CFU between individuals. The residual variability was described by two additive components (on log-scale), one shared by all replicates and one shared between replicates from the same sputum sample. Final parameter estimates are listed in **Table 2**.

The final model described the patient data well, according to the prediction-corrected visual predictive checks (**Figure 2**). The estimated second-order death rates were 0.200 and 0.106 $L \cdot mg^{-1} \cdot days^{-1}$ for the slow- and nonmultiplying states, respectively. The inhibition of fast-multiplying growth was estimated close to 1 (100%) and was therefore be fixed to 1 in the final model with no change in OFV. The model predicted a gradient of decline in CFU with dose (**Figure 3a**). In **Figure 3b**, the typical model predicted bacterial number over time is seen for different states. External validation revealed the ability of the final MTP model to predict data from other sources well without any re-estimation (**Figure 4**). Simulations using the alternative two-state model without a nonmultiplying state did not predict external data well (**Figure 5**).

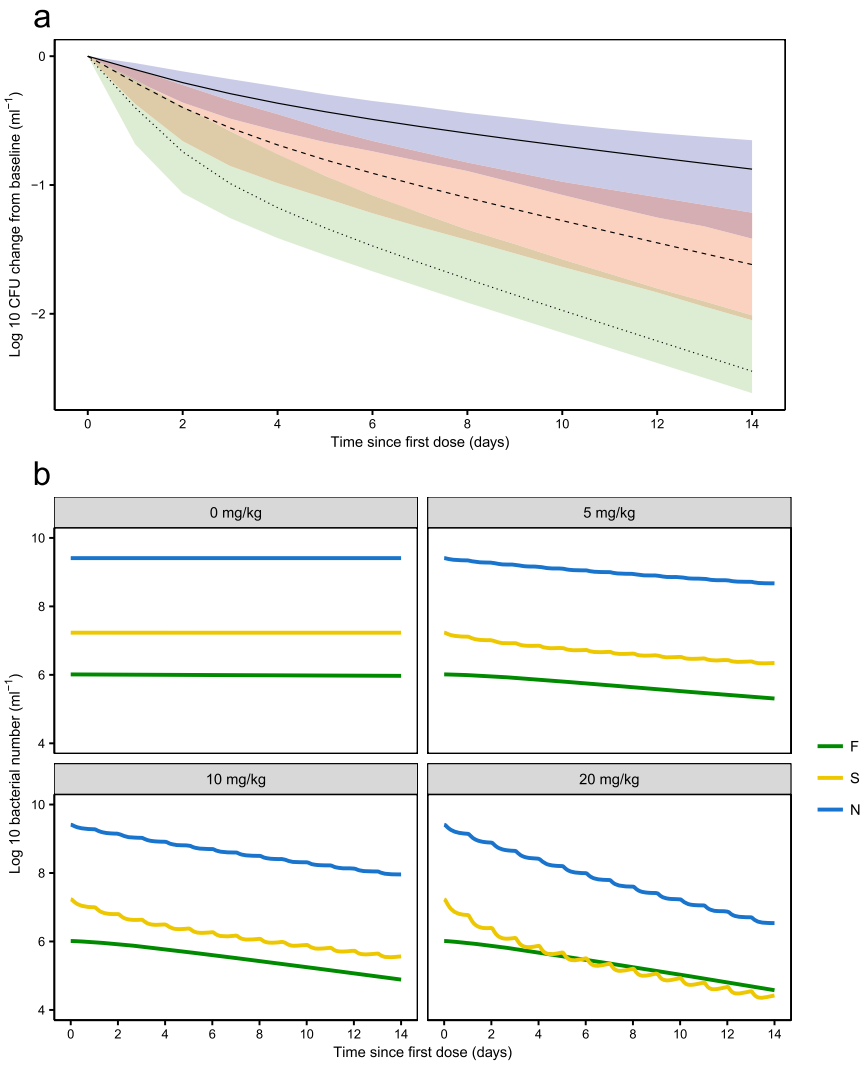


**Figure 3** Typical model predictions from the final Multistate Tuberculosis Pharmacometric model of (**a**) log-10 change from baseline in colony forming unit (CFU) after daily rifampicin doses of 5 mg/kg body weight (solid black line, blue shaded area is the 95% prediction interval [PI], including model uncertainty), 10 mg/kg body weight (dashed black line, red shaded area is the 95% PI, including model uncertainty), and 20 mg/kg body weight (dotted black line, green shaded area is the 95% PI, including model uncertainty) and (**b**) model predicted typical bacterial number of the fast- (green), slow- (yellow), and nonmultiplying (blue) states, denoted F, S, and N, respectively, following different daily doses of rifampicin per kg body weight.

## DISCUSSION

The MTP model can be applied to clinical data with only re-estimation of the $B_{max}$ parameter and estimation of the exposure-response relationships for rifampicin. Other MTP model parameters can be fixed to estimates obtained from fitting the model to *in vitro* data.[15] The external validation showed the ability of the final model to predict change in CFU after different rifampicin doses (**Figure 4**).

All patients were assumed to have stationary phase infections. Time of onset of symptoms and trial entry were unknown. A suggested incubation period is 1.26 years.[29] However, at that time, patients are in the stationary phase with negligible change in CFU with respect to time. For computational simplicity, the time of entering trial was assumed to 150 days, a time point at which the model predicts negligible change in CFU in the stationary phase.

In order to account for different baseline sputum CFU values in the *in vitro* and clinical settings, $B_{max}$ was re-estimated. Re-estimation of $B_{max}$ did not affect the relative amounts of bacterial states. The relative amounts are determined by the rates between states that were fixed to *in vitro* estimates.[15] In the *in vitro* system, transfer from non- to fast-multiplying state was excluded because of hypoxia. In contrast, clinical lesions might have partial access to oxygen. However, the transfer might be suppressed clinically by the immune system. In the *in vitro* model, there is a time-dependent transfer between fast- and slow-multiplying bacteria,[15] which has not been validated *in vivo* because of clinical data not being informative

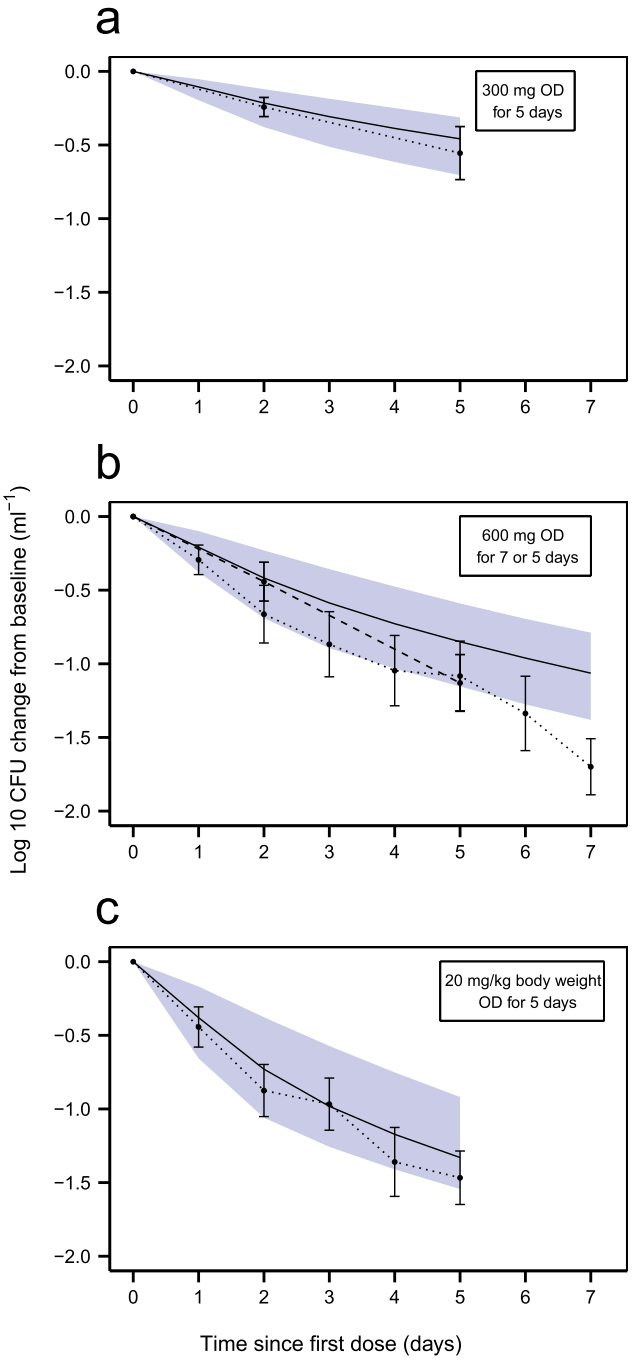


**Figure 4** Clinical trial simulations using the final Multistate Tuberculosis Pharmacometric model. Log-10 colony forming unit (CFU) in mL$^{-1}$ change from baseline vs. time since first dose of rifampicin for (**a**) 300 mg of rifampicin given once daily (OD) for 5 days[28]; (**b**) 600 mg rifampicin given OD for 5 (dashed line) and 7 (dotted line) days[26,27]; (**c**) 20 mg rifampicin per kg body weight given OD for 5 days.[27] Shaded areas are the 95% confidence interval for the typical prediction of log-10 CFU (mL$^{-1}$) change from baseline vs. time since first dose from 1,000 samples simulated with parameter uncertainty. Solid lines are the typical predictions from the final model for the study design indicated in the top right box in each graph. Dots are the mean values at each designated time point with SEs shown as error bars. The dots are connected with dotted and/or dashed lines.

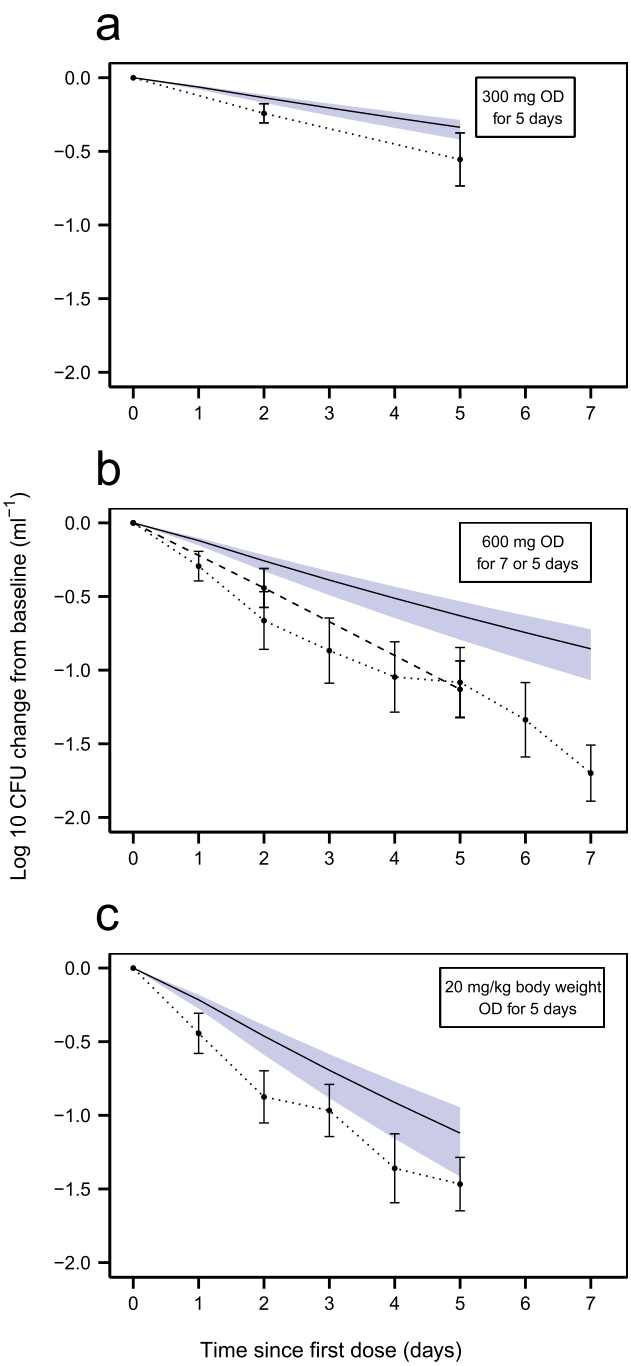


**Figure 5** Clinical trial simulations using an alternative two-state model without inclusion of a nonmultiplying state. Log-10 colony forming unit (CFU) in mL$^{-1}$ change from baseline vs. time since first dose of rifampicin for (**a**) 300 mg of rifampicin given once daily (OD) for 5 days[28]; (**b**) 600 mg rifampicin given OD for 5 (dashed line) and 7 (dotted line) days[26,27]; (**c**) 20 mg rifampicin per kg body weight given OD for 5 days.[27] Shaded areas are the 95% confidence interval for the typical prediction of log-10 CFU (mL$^{-1}$) change from baseline vs. time since first dose from 1,000 samples simulated with parameter uncertainty. Solid lines are the typical predictions from the model without a nonmultiplying state for the study design indicated in the top right box in each graph. Dots are the mean values at each designated time point with SEs shown as error bars. The dots are connected with dotted and/or dashed lines.

enough. There might be strain differences between the *in vitro* H37Rv strain data used to develop the MTP model and clinical strains. The most important difference would be the drug susceptibility. However, all exposure-response parameters were estimated in this work using the clinical data. Growth- and transfer rates between substates were fixed to estimates from the *in vitro* model, which might deviate from clinical strains, but did not seem to affect the overall ability to predict external data as such (**Figure 4**).

A limitation of this analysis was that no PK information was available. However, a population PK parameter approach[20] was used, which does not require PK information but is reusing a previously developed population PK model.[19] As no IIV or covariate information were included in the PK model, IIV in exposure-response parameters was not evaluated as it would most likely represent a sum of PK and pharmacodynamic (PD) variability. Only IIV in $B_{max}$ was estimated, which allowed for prediction of different CFU baseline levels. One assumption in the population PK parameter approach is that the typical patient in the dataset used for developing the population PK model is representative for a typical patient in the PD dataset. Because covariates for the PD dataset were unknown, it is difficult to judge the impact of this assumption. The PK model applied was developed using patient data from South Africa, Benin, Senegal, and Guinea,[19] whereas the patients included in this analysis originated from Kenya. Rifampicin exposure has been shown to be slightly higher in eastern Africa.[30] Our analysis relies on a small historical dataset, which may not reflect current TB trials. However, the final model predicted recent trials (**Figure 4**) justifying the approach and data used despite these discrepancies.

We investigated the immune system as a bactericidal process but no immune effect was supported that might be due to the limited study duration. Most information regarding this parameter was available in the negative control group.

The final model predicted a gradient of reduction in CFU with increasing dose (**Figure 3a**). Bowness *et al.*[31] compared matched CFU counts with time to positivity in mycobacterial growth incubator tube in rifampicin-treated patients in which mycobacterial growth incubator tube quantifies a subpopulation unable to grow on solid media. Rifampicin had a dose-dependent activity against this subpopulation that we believe coincides with the drug effect on the nonmultiplying state seen here. The predicted potency was higher toward slow- than nonmultiplying bacteria (**Table 2**). No drug effect was supported regarding death of fast-multiplying state, contradicting that fast-multiplying subpopulations are more susceptible to drug exposure.[14] However, the fast-multiplying bacteria might have been too few in the stationary phase patients in order to find any significant drug effect or there was an indistinguishable balance between kill and inhibition of growth.

In **Figure 3b**, the typical model predicted bacterial number over time is seen for the different subpopulations. The change in slow- and nonmultiplying states is circadian because of the direct effect by the drug through the link to plasma concentration. As the model included no concentration-dependent effect on fast-multiplying bacteria, but only complete inhibition of the growth of fast-multiplying bacteria, no circadian change is seen for this state.

The model predicted high numbers of unquantifiable bacteria (i.e., nonmultiplying state), as inherited from the *in vitro* model.[15] *In vitro*, animal and clinical studies support *M. tuberculosis* subpopulation(s) that are culture-negative on solid media but can grow in liquid media.[32–34]

The final MTP model was compared to a two-state model, not including a nonmultiplying state. The OFV was lower ($\Delta$OFV $= -4.19$) for the final MTP model compared to the two-state model without a nonmultiplying state. The latter model predicted a net decline in CFU in the stationary phase that did not agree with the negative control group. Noncultivable subpopulations have been described in PK/PD models for malaria[35,36] and *Escherichia coli*.[37] There are several empirical CFU models for TB,[9,11,38,39] but none are semimechanistic like the MTP model, which links PK to multiple mycobacterial states.

The sputum sampling compartment method was chosen to handle predictions of CFU that best resembled the sample collection procedure compared with the other methods investigated. Sampling intervals, time points for sampling, and sample volumes can deviate within and between studies, which can be accounted for using our approach (**Supplementary Material S1 and S2**). Patients produce less sputum as treatment progresses, which could be important to account for in future analyses.[21] Variability in CFU is also affected, as it increases at smaller sample volumes. Larger sputum volumes can be obtained (e.g., by increasing the sampling interval),[40] which could be accounted for using our approach. The assumed volume of 10 mL will not affect the predictions because the model predicts the average bacterial number over the sampling interval. Assuming higher volumes would be compensated by a higher sputum production rate.

In addition to the clinical application presented here, the MTP model has been successfully applied to *in vitro*[15] and mouse data.[16] As such, the MTP model can be used for analysis and simulation of clinical and preclinical trials within TB drug development to optimize the development of drugs against TB.

In summary, the MTP model was successfully applied to clinical data with rifampicin-treated patients. Retrospective data were successfully predicted using this approach.

**ACKNOWLEDGMENTS.** The research leading to these results has received funding from the Swedish Research Council in addition to the Innovative Medicines Initiative Joint Undertaking (www.imi.europe.eu) under grant agreement number 115337, resources of which are composed of financial contribution from the European Union's Seventh Framework Programme (FP7/2007-2013) and EFPIA companies' in kind contribution. The authors are grateful for the sharing of data by Dr. Amina Jindani.

## CONFLICT OF INTEREST

The authors declared no conflict of interest.

## AUTHOR CONTRIBUTIONS

R.J.S. and U.S.H.S. wrote the manuscript. R.J.S. and U.S.H.S. designed the research. R.J.S. and U.S.H.S. analyzed the data.

1. World Health Organization. *Treatment of tuberculosis: guidelines for national programmes* 4th ed. (Global Tuberculosis Programme, World Health Organization, Geneva, Switzerland, 2009).
2. Mitchison, D.A. Role of individual drugs in the chemotherapy of tuberculosis. *Int. J. Tuberc. Lung Dis.* **4**, 796–806 (2000).
3. Wehrli, W., Knüsel, F., Schmid, K. & Staehelin, M. Interaction of rifamycin with bacterial RNA polymerase. *Proc. Natl. Acad. Sci. USA* **61**, 667–673 (1968).
4. Harshey, R.M. & Ramakrishnan, T. Rate of ribonucleic acid chain growth in Mycobacterium tuberculosis H37Rv. *J. Bacteriol.* **129**, 616–622 (1977).
5. Coates, A.R. & Hu, Y. Targeting non-multiplying organisms as a way to develop novel antimicrobials. *Trends Pharmacol. Sci.* **29**, 143–150 (2008).
6. Vynnycky, E. & Fine, P.E. Lifetime risks, incubation period, and serial interval of tuberculosis. *Am. J. Epidemiol.* **152**, 247–263 (2000).
7. Sirgel, F., Venter, A. & Mitchison, D. Sources of variation in studies of the early bactericidal activity of antituberculosis drugs. *J. Antimicrob. Chemother.* **47**, 177–182 (2001).
8. Mukamolova, G.V., Turapov, O., Malkin, J., Woltmann, G. & Barer, M.R. Resuscitation-promoting factors reveal an occult population of tubercle Bacilli in sputum. *Am. J. Respir. Crit. Care Med.* **181**, 174–180 (2010).
9. Jindani, A., Doré, C.J. & Mitchison, D.A. Bactericidal and sterilizing activities of antituberculosis drugs during the first 14 days. *Am. J. Respir. Crit. Care Med.* **167**, 1348–1354 (2003).
10. Perrin, F.M., Lipman, M.C., McHugh, T.D. & Gillespie, S.H. Biomarkers of treatment response in clinical trials of novel antituberculosis agents. *Lancet Infect. Dis.* **7**, 481–490 (2007).
11. Sloan, D.J. *et al.* Pharmacodynamic modeling of bacillary elimination rates and detection of bacterial lipid bodies in sputum to predict and understand outcomes in treatment of pulmonary tuberculosis. *Clin. Infect. Dis.* **61**, 1–8 (2015).
12. Wayne, L.G. & Hayes, L.G. An in vitro model for sequential study of shiftdown of Mycobacterium tuberculosis through two stages of nonreplicating persistence. *Infect. Immun.* **64**, 2062–2069 (1996).
13. Tuomanen, E. Phenotypic tolerance: the search for beta-lactam antibiotics that kill nongrowing bacteria. *Rev. Infect. Dis.* **8** Suppl 3, S279–S291 (1986).
14. Coates, A., Hu, Y., Bax, R. & Page, C. The future challenges facing the development of new antimicrobial drugs. *Nat. Rev. Drug Discov.* **1**, 895–910 (2002).
15. Clewe, O., Aulin, L., Hu, Y., Coates, A.R. & Simonsson, U.S. A multistate tuberculosis pharmacometric model: a framework for studying anti-tubercular drug effects in vitro. *J. Antimicrob. Chemother.* **71**, 964–974 (2016).
16. Chen, C. *et al.* Semi-mechanistic pharmacokinetic-pharmacodynamic modeling of rifampicin treatment response in a tuberculosis acute mouse model. Washington, DC, 5–9 September 2014, Abstract A-024. <http://www.icaaconline.com/php/icaac2014abstracts/data/papers/2014/A-024.htm>.
17. Jindani, A., Aber, V.R., Edwards, E.A. & Mitchison, D.A. The early bactericidal activity of drugs in patients with pulmonary tuberculosis. *Am. Rev. Respir. Dis.* **121**, 939–949 (1980).
18. Beal, S., Sheiner, L.B., Boeckmann, A. & Bauer, R.J. NONMEM user's guides (1989–2013). Icon Development Solutions, Ellicott City, MD, 2013.
19. Smythe, W. *et al.* A semimechanistic pharmacokinetic-enzyme turnover model for rifampin autoinduction in adult tuberculosis patients. *Antimicrob. Agents Chemother.* **56**, 2091–2098 (2012).
20. Zhang, L., Beal, S.L. & Sheiner, L.B. Simultaneous vs. sequential analysis for population PK/PD data I: best-case performance. *J. Pharmacokinet. Pharmacodyn.* **30**, 387–404 (2003).
21. Karinja, M.N., Esterhuizen, T.M., Friedrich, S.O. & Diacon, A.H. Sputum volume predicts sputum mycobacterial load during the first 2 weeks of antituberculosis treatment. *J. Clin. Microbiol.* **53**, 1087–1091 (2015).
22. Keizer, R.J., Karlsson, M.O. & Hooker, A. Modeling and simulation workbench for NONMEM: tutorial on Pirana, PsN, and Xpose. *CPT Pharmacometrics Syst. Pharmacol.* **2**, e50 (2013).
23. Xpose software. <http://xpose.sourceforge.net/>. Accessed 11 November 2014.
24. Bergstrand, M., Hooker, A.C., Wallin, J.E. & Karlsson, M.O. Prediction-corrected visual predictive checks for diagnosing nonlinear mixed-effects models. *AAPS J.* **13**, 143–151 (2011).
25. PsN software. <http://psn.sourceforge.net/>. Accessed 11 November 2014.
26. Rustomjee, R. *et al.* Early bactericidal activity and pharmacokinetics of the diarylquinoline TMC207 in treatment of pulmonary tuberculosis. *Antimicrob. Agents Chemother.* **52**, 2831–2835 (2008).
27. Diacon, A.H. *et al.* Early bactericidal activity of high-dose rifampin in patients with pulmonary tuberculosis evidenced by positive sputum smears. *Antimicrob. Agents Chemother.* **51**, 2994–2996 (2007).
28. Sirgel, F.A. *et al.* The early bactericidal activities of rifampin and rifapentine in pulmonary tuberculosis. *Am. J. Respir. Crit. Care Med.* **172**, 128–135 (2005).
29. Borgdorff, M.W., Sebek, M., Geskus, R.B., Kremer, K., Kalisvaart, N. & van Soolingen, D. The incubation period distribution of tuberculosis estimated with a molecular epidemiological approach. *Int. J. Epidemiol.* **40**, 964–970 (2011).
30. Tostmann, A. *et al.* Pharmacokinetics of first-line tuberculosis drugs in Tanzanian patients. *Antimicrob. Agents Chemother.* **57**, 3208–3213 (2013).
31. Bowness, R. *et al.* The relationship between Mycobacterium tuberculosis MGIT time to positivity and cfu in sputum samples demonstrates changing bacterial phenotypes potentially reflecting the impact of chemotherapy on critical sub-populations. *J. Antimicrob. Chemother.* **70**, 448–455 (2015).
32. Hu, Y. *et al.* Detection of mRNA transcripts and active transcription in persistent Mycobacterium tuberculosis induced by exposure to rifampin or pyrazinamide. *J. Bacteriol.* **182**, 6358–6365 (2000).
33. Dhillon, J., Lowrie, D.B. & Mitchison, D.A. Mycobacterium tuberculosis from chronic murine infections that grows in liquid but not on solid medium. *BMC Infect. Dis.* **4**, 51 (2004).
34. Dhillon, J., Fourie, P.B. & Mitchison, D.A. Persister populations of Mycobacterium tuberculosis in sputum that grow in liquid but not on solid culture media. *J. Antimicrob. Chemother.* **69**, 437–440 (2014).
35. Svensson, U.S., Alin, H., Karlsson, M.O., Bergqvist, Y. & Ashton, M. Population pharmacokinetic and pharmacodynamic modelling of artemisinin and mefloquine enantiomers in patients with falciparum malaria. *Eur. J. Clin. Pharmacol.* **58**, 339–351 (2002).
36. Hietala, S.F. *et al.* Population pharmacokinetics and pharmacodynamics of artemether and lumefantrine during combination treatment in children with uncomplicated falciparum malaria in Tanzania. *Antimicrob. Agents Chemother.* **54**, 4780–4788 (2010).
37. Khan, D.D. *et al.* A mechanism-based pharmacokinetic/pharmacodynamic model allows prediction of antibiotic killing from MIC values for WT and mutants. *J. Antimicrob. Chemother.* **70**, 3051–3060 (2015).
38. Gillespie, S.H., Gosling, R.D. & Charalambous, B.M. A reiterative method for calculating the early bactericidal activity of antituberculosis drugs. *Am. J. Respir. Crit. Care Med.* **166**, 31–35 (2002).
39. Rustomjee, R. *et al.* A phase II study of the sterilising activities of ofloxacin, gatifloxacin and moxifloxacin in pulmonary tuberculosis. *Int. J. Tuberc. Lung Dis.* **12**, 128–138 (2008).
40. Hafner, R. *et al.* Early bactericidal activity of isoniazid in pulmonary tuberculosis. Optimization of methodology. The DATRI 008 Study Group. *Am. J. Respir. Crit. Care Med.* **156**(3 Pt 1), 918–923 (1997).



Supplementary information accompanies this paper on the *CPT: Pharmacometrics & Systems Pharmacology* website (http://www.wileyonlinelibrary.com/psp4)